# Synthetic, Electrochemical, Optical, and Conductivity Studies of Coordination Polymers of Iron, Ruthenium, and Osmium Octaethylporphyrin

**James P. Collman,*[1a] John T. McDevitt,[1a] Charles R. Leidner,[1a,b] Gordon T. Yee,[1a] Jerry B. Torrance,[1c] and William A. Little[1d]**

*Contribution from the Departments of Chemistry and Physics, Stanford University, Stanford, California 94305, and IBM Research Labs, Almaden Research Center, 650 Harry Road K32-803, San Jose, California 95120-6099.* *Received November 17, 1986*

**Abstract:** A series of ligand-bridged metalloporphyrin polymers, $[M(OEP)(L\text{-}L)]_n$ (M = Fe, Ru, Os; L-L = pyrazine, 4,4′-bipyridine, 1,4-diazabicyclo[2.2.2]octane), have been synthesized and characterized. When partially oxidized, these polymers are highly conductive. The conductivity of these polymers depends on the extent of doping, the nature of the central transition metal, and the bridging ligand. The doped polymers exhibit strong infrared absorptions due to mixed-valence transitions, the features of which correlate with the bulk conductivity. The infrared spectra of the doped $[Os(OEP)(pyz)]_n$ samples reveal the presence of a coupling between an IR-silent vibrational mode of the bridging ligand and a mixed-valence transition, which suggests that the bridging ligand participates in the conduction process. Electrochemical studies of the polymers have been carried out with carbon cloth electrodes. These studies demonstrate that the doping reactions are metal-centered and corroborate the assertion that the porphyrin $\pi$-electrons are not involved in the conduction pathway. This feature contrasts with most of the previous work with porphyrinic conductors in which the conduction pathway is dominated by the macrocycle.

Over the last two decades, the search for conductive polymers and molecular metals has blossomed into an interdisciplinary endeavor which now finds researchers studying a wide variety of systems,[2] including purely organic polymers, stacked and bridged stacked inorganic complexes, and organic charge-transfer salts. Many of these systems exhibit novel optical, magnetic, electronic, and conductive properties. Several of these materials have been shown to have useful applications, including a switchable ion conducting membrane,[3] photovoltaic devices based on polyacetylene[4] and $(SN)_x$ films,[5] current and optical-switching in thin films of CuTCNQ (TCNQ = tetracyanoquinodimethane),[6] high density rechargable batteries,[7] molecular-based electronic devices,[8] stabilization of *n*-type silicon photoelectrochemical cells,[9] and controlled release of drugs from microelectrodes.[10]

The chemical versatility of metalloporphyrin and related macrocyclic complexes provides an opportunity to prepare a large matrix of conductive materials.[11] Their high chemical and thermal stability, their ability to complex both main-group and transition metals, and their propensity to form cofacial stacks makes porphyrinic complexes attractive candidates for conductive systems. Porphyrinic molecular metals can be grouped into two classes: (1) stacked and (2) bridged macrocyclic conductors. Ni(Pc)I (Pc = phthalocyanine), Ni(tbp)I (tbp = tetrabenzoporphyrin), Ni(tmp)I (tmp = *meso*-tetramethylporphyrin), and $Ni(omtbp)I_{1.08}$ (omtbp = octamethyltetrabenzoporphyrin)[11] typify the former class while $[M(Pc)O]_n$ (M = Si, Ge, Sn) and $[M(Pc)F]_n$ (M = Al, Ga) exemplify the latter class.[12] Both the extended ligand-based $\pi$-systems and metal orbitals of porphyrinic complexes can participate in the conduction process. In most of the past work with these systems, $\pi$-electrons from the macrocycle were involved in the conduction process, although ESR studies of Ni(tbp)I have indicated that a small spin component resides on the metal in this complex.[11] Hanack et al. have prepared a large family of bridged coordination polymers employing macrocyclic ligands of the type $[M(Pc)(L\text{-}L)]_n$ where M = Fe, Ru, Co, or Rh and L-L = pyrazine, 4,4′-bipyridine, *s*-tetrazine, or 1,4-diisocyanobenzene.[13] The authors have implied that both the transition metal and the bridging ligand are involved in the conduction pathway. However, a thorough study of $[Fe(Pc)(pyz)]_n$ by $^{57}Fe$ Mössbauer and ESR spectroscopy suggests that oxidation of this polymer during p-doping occurs mainly at the macrocycle.[13c] Studies of the conduction pathway in the other systems have not yet been reported.

Hoffman and Ibers have recently reported the first authenticated example of a stacked macrocyclic system, CoPcI, in which the metal spine supports the conduction.[14] An important extension of this work would involve the preparation of heavy transition-metal macrocyclic complexes in which the larger radial extension

(1) (a) Chemistry Department, Stanford University. (b) Present address: Department of Chemistry, Purdue University, West Lafayette, IN 47907. (c) IBM Almaden Research Labs. (d) Stanford University, Physics Department.

(2) (a) "Proceedings of the Workshop on Synthetic Metals": *Synthetic Met.* **1984**, *9*, 129-346. (b) "Proceedings of the International Conference on Synthetic Metals"; Labes, U. U., Ed. *Mol. Cryst. Liq. Cryst.* **1985**, *Vol. 117-121*, parts A-E. (c) *Handbook on Conducting Polymers*; Skotheim, T. J., Ed., Marcel Dekker: New York, in press. (d) Comes, R.; Bernier, P.; Andre, J. J.; Rouxel, J. *Proceedings of the International Conference on Low Dimensional Conductors and Superconductors*; Les Arcs-Bourg-Saint-Maurice-Savoie: France, Dec 1982 (*J. Phys., Colloq.* **1983**, C3). (e) Miller, J. S., Ed. *Extended Linear Chain Compounds*; Plenum: New York, 1982; Vols. 1-3.

(3) (a) Burgmayer, P.; Murray, R. W. *J. Electroanal. Chem.* **1983**, *147*, 339-344. (b) Burgmayer, P.; Murray, R. W. *J. Phys. Chem.* **1984**, *88*, 2515-2521.

(4) (a) Tsukamoto, J.; Ohigashi, H.; Matsumura, K.; Takahashi, A. *Synth. Metals* **1982**, *4*, 177-186. (b) Weinberger, B. R.; Akhtar, M.; Gan, S. C. *Synth. Met.* **1982**, *4*, 187-197.

(5) Cohen, M. J.; Harris, J. S. *Appl. Phys. Lett.* **1978**, *33*, 812-814.

(6) Potember, R. S.; Poehler, T. O.; Benson, R. C. *Appl. Phys. Lett.* **1982**, *41*, 548-550.

(7) (a) Nigrey, J. P.; MacDiarmid, A. G.; Heeger, A. J. *Mol. Cryst. Liq. Cryst.* **1982**, *83*, 1341-1349. (b) Kaneto, K.; Maxfield, M.; Nairns, D. P.; MacDiarmid, A. G.; Heeger, A. J. *J. Chem. Soc., Faraday Trans. 1* **1982**, *78*, 3417-3429. (c) Shacklette, L. W.; Elsenbaumer, R. L.; Chance, R. R.; Sowa, J. M.; Ivory, D. M.; Miller, G. C.; Baughman, R. H. *J. Chem. Soc., Chem. Commun.* **1982**, *6*, 361-362.

(8) (a) Chidsey, C. E. D.; Murray, R. W. *Science (Washington, D.C.)* **1986**, *231*, 25-31. (b) Kittleson, G. P.; White, H. S.; Wrighton, M. S. *J. Am. Chem. Soc.* **1984**, *106*, 7389-7396.

(9) Frank, A. J.; Honda, K. *J. Phys. Chem.* **1982**, *86*, 1933-1935.

(10) Zinger, B.; Miller, L. L. *J. Am. Chem. Soc.* **1984**, *106*, 6861-6863.

(11) Hoffman, B. M.; Ibers, J. A. *Acc. Chem. Res.* **1983**, *16*, 15-21.

(12) (a) Dirk, C. W.; Inabe, T.; Schoch, K. F., Jr.; Marks, T. J. *J. am. Chem. Soc.* **1983**, *105*, 1539-1550. (b) Joyner, R. D.; Kenney, M. E. *J. Am. Chem. Soc.* **1960**, *82*, 5790-5791. (c) Nohr, R. S.; Kuznesof, P. M.; Wynne, K. J.; Kenney, M. E.; Siebenman, P. G. *J. Am. Chem. Soc.* **1981**, *103*, 4371-4377. (d) Wynne, K. J.; Nohr, R. S. *Mol. Cryst. Liq. Cryst.* **1981**, *81*, 243-254.

(13) (a) Schneider, O.; Hanack, M. *Mol. Cryst. Liq. Cryst.* **1982**, *81*, 273-284 and references therein. (b) Hanack, M. *Mol. Cryt. Liq. Cryst.* **1984**, *105*, 133-149. (c) Diel, B. N.; Inabe, T.; Taggi, N. K.; Lyding, J. W.; Schneider, O.; Hanack, M.; Kannewurf, C. R.; Marks, T. J.; Schwartz, L. H. *J. Am. Chem. Soc.* **1984**, *106*, 3207-3214.

(14) Martinsen, J.; Stanton, J. L.; Greene, R. L.; Tanaka, J.; Hoffman, B. M.; Ibers, J. A. *J. Am. Chem. Soc.* **1985**, *107*, 6915-6920.

0002-7863/87/1509-4606$01.50/0 

of the metal orbitals should result in greater overlap. Very little research has been done in this area because the chemistry of heavy metal porphyrins has been developed only recently.

Collman et al. have previously reported[15] the synthesis and characterization of a series of neutral metalloporphyrin dimers of the types $[M(OEP)]_2$ and $[M(TTP)]_2$ (where OEP = octaethylporphyrin and TTP = tetratolylporphyrin) for M = Ru, Os, or Mo. These complexes are linked by metal–metal bonds between the central transition metals. The neutral metalloporphyrin dimers of ruthenium and osmium possess a bond order of 2 and the Mo dimer a bond order of 4. It has been demonstrated that the neutral ruthenium and osmium porphyrin dimers can be oxidized by one or two electrons with retention of their dimeric structure to produce complexes having bond orders of 2.5 and 3, respectively.[16]

These ruthenium and osmium metalloporphyrin dimers have proved to be particularly useful synthons because they may be cleaved with a variety of coordinating ligands to produce the bis-ligand monomers (eq 1–3).[17] A logical extension of this theme

$$^1/_2[M(OEP)]_2 + 2THF \xrightarrow{\text{days}} M(OEP)(THF)_2 \quad (1)$$

$$^1/_2[M(OEP)]_2 + 2py \xrightarrow{\text{minutes}} M(OEP)(py)_2 \quad (2)$$

$$^1/_2[M(OEP)]_2 + 2CO \xrightarrow{\text{seconds}} M(OEP)(CO)_2 \quad (3)$$

$$M = Ru, Os$$

is the use of neutral bridging ligands to produce polymeric structures (eq 4). This general reaction scheme could lead to

$$^1/_2[M(OEP)]_2 + L\text{-}L \rightarrow [M(OEP)(L\text{-}L)]_n \quad (4)$$

a large matrix of possible coordination polymers. In principle, with the proper choice of M, L-L, and metal oxidation level, a range of optical, magnetic, and conductive properties might be tailored into such systems.

Ruthenium(II) and osmium(II) complexes are particularly good choices of building blocks for conductive polymers. Extensive work by Taube et al. has shown that mixed-valence dimers of Ru and Os possess electrons that are easily delocalized through bridging $\pi$-acid ligands.[18] Furthermore, due to the largely nonbonding character of these electrons, the coordination sphere of the metal is not appreciably changed by one-electron oxidation. Thus, oxidative doping of polymers employing these transition metals should result in minimal changes in the coordination properties of the polymer backbone. Therefore the formation of trapping centers (polarons) that limit carrier mobility should be minimized.

Recently we have developed methods for the synthesis of polymeric metalloporphyrin analogues of Taube's mixed-valence dimers. Our initial studies[19] focused on pyrazine- (pyz-) bridged polymers of iron, ruthenium, and osmium octaethylporphyrin. Here, we expand this group to include 1,4-diazabicyclo[2.2.2]-octane (dabco) and 4,4′-bipyridine (bpy) coordination polymers of ruthenium and osmium octaethylporphyrin. The optical, electron transport, and electrochemical properties of all these materials are presented herein.

## Experimental Section

**General Methods.** All manipulations were carried out in an oxygen-free, nitrogen-filled Vacuum Atmospheres glovebox (Hawthorne, California), in Schlenkware, or on a high vacuum line. Solvents were purified, dried and degassed according to literature procedures.[20] 4,4′-Bipyridine, pyrazine, dabco, and octaethylporphyrin were obtained from Aldrich Chemical Co., and pyrazine-$d_4$ was obtained from Cambridge Isotopes Laboratory, Cambridge, MA. 4,4′-Bipyridine was recrystallized twice from ethyl acetate and dried in a vacuum oven at 70 °C. All other chemicals were reagent grade and were used without further purification. Elemental analyses were performed by Chemical Analytical Services, Berkeley, CA. Bis[(octaethylporphyrinato)ruthenium(II)], $[Ru(OEP)]_2$, and bis[(octaethylporphyrinato)osmium(II)], $[Os(OEP)]_2$, were prepared according to literature procedures.[15] (Octaethylporphyrinato)bis(pyrazine)ruthenium(II), $Ru(OEP)(pyz)_2$, (octaethylporphyrinato)bis(pyrazine)osmium(II), $Os(OEP)(pyz)_2$, ($\mu$-pyrazine)(octaethylporphyrinato)-ruthenium(II), $[Ru(OEP)(pyz)]_n$, ($\mu$-pyrazine)(octaethylporphyrinato)-osmium(II), $[Os(OEP)(pyz)]_n$, and their pyrazine-$d_4$ analogues were prepared with use of previously reported procedures.[19a]

**($\mu$-1,4-Diazabicyclo[2.2.2]octane)(octaethylporphyrinato)ruthenium(II), $[Ru(OEP)(dabco)]_n$ (1).** In the glovebox, $[Ru(OEP)]_2$ (0.054 g, 0.043 mmol) was dissolved in 15 mL of toluene. To this solution was added 0.086 mmol of dabco from a stock solution. Although a light brown precipitate formed immediately, the reaction was stirred for an additional 24 h at room temperature to promote uniformly high molecular weights. The product was collected on a fritted disk, washed with toluene and hexanes, and dried under vacuum ($10^{-6}$ torr) at 60 °C overnight: yield 0.048 g, 76% based on porphyrin content; UV–vis/near-IR (Fluorolube mull) ($\lambda_{max}$, nm) 390 (Soret), 490, 518; IR ($\bar{\nu}$, $cm^{-1}$) (Fluorolube) 2960 (vs), 2928 (s), 2868 (s), 1677 (w), 1594 (vw), 1545 (m), 1467 (s), 1450 (m), 1380 (m), 1372 (m), 1364 (m). Anal. Calcd for $C_{42}H_{56}N_6Ru$: C, 67.61; H, 7.56; N, 11.26. Found: C, 67.41; H, 7.67; N, 11.06.

**($\mu$-1,4-Diazabicyclo[2.2.2]octane)(octaethylporphyrinato)osmium(II), $[Os(OEP)(dabco)]_n$ (2).** In a fashion similar to that described for $[Ru(OEP)(dabco)]_n$, $[Os(OEP)]_2$ (0.077 g, 0.054 mmol) in 30 mL of toluene was allowed to react with dabco (0.108 mmol). A purple-brown precipitate began to form after 5 min of stirring. After 24 h the product was isolated as described above: yield 0.079 g, 88%; UV–vis/near-IR (Fluorolube mull) ($\lambda_{max}$, nm) 360 (Soret), 560, 618, 880; IR ($\bar{\nu}$, $cm^{-1}$) (Fluorolube) 2960 (vs), 2929 (s), 2868 (s), 1661 (w), 1590 (vw), 1539 (w), 1476 (w), 1463 (ms), 1446 (m), 1391 (w), 1372 (ms), 1362 (w). Anal. Calcd for $C_{42}H_{56}N_6Os$: C, 60.40; H, 6.76; N, 10.06. Found: C, 60.01; H, 6.39; N, 9.63.

**($\mu$-4,4′-Bipyridine)(octaethylporphyrinato)ruthenium(II), $[Ru(OEP)(bpy)]_n$ (3), and ($\mu$-4,4′-Bipyridine)(octaethylporphyrinato)osmium(II), $[Os(OEP)(bpy)]_n$ (4).** In a fashion similar to that described for the dabco-bridged polymers **1** and **2**, $[Ru(OEP)(bpy)]_n$ was prepared by treating $[Ru(OEP)]_2$ (0.045 g, 0.035 mmol) with 4,4′-bipyridine (0.070 mmol) in 15 mL of toluene. After the solution was stirred 10 min at room temperature, an insoluble blue powder formed. Stirring was continued for 24 h, and the product was collected: yield 0.052 g, 96%; UV–vis/near-IR (Fluorolube mull) ($\lambda_{max}$, nm) 390 sh, 410 (Soret), 500, 530, 750 sh, 770; IR ($\bar{\nu}$, $cm^{-1}$) (Flurolube) 2956 (vs), 2927 (s), 2864 (s), 1673 (w), 1592 (w), 1543 (mw), 1512 (w), 1482 (vs), 1465 (m), 1447 (m), 1421 (w), 1375 (m), 1362 (w). Anal. Calcd for $C_{46}H_{52}N_6Ru$: C, 69.93; H, 6.63; N, 10.63. Found: C, 70.12; H, 6.72; N, 10.54.

Likewise, $[Os(OEP)]_2$ (0.081 g, 0.056 mmol) was treated with 4,4′-bipyridine (0.112 mmol) in 40 mL of toluene. After 1 h of stirring at room temperature, a purple powder began to precipitate. The reaction was heated at reflux for an additional 16 h at which time the product was isolated: yield 0.099 g, 100%; UV–vis/near-IR (flurolube mull) ($\lambda_{max}$, nm) 390 (Soret), 525, 590 sh, 760, 1010; IR ($\bar{\nu}$, $cm^{-1}$) (flurolube) 2956 (vs), 2929 (s), 2856 (s), 1674 (w), 1605 (w), 1590 (w), 1544 (m), 1479 (vs), 1446 (m), 1422 (w), 1381 (m), 1374 (m), 1362 (m). Anal. Calcd for $C_{46}H_{52}N_6Os$: C, 62.84; H, 5.96; N, 9.56. Found: C, 62.57, H, 5.91; N, 9.39.

**Doping of the Coordination Polymers.** Doping reactions employing $I_2$ and $NOPF_6$ (nitrosyl hexafluorophosphate) were performed as described previously.[19] With ferricinium hexafluorophosphate $[Fe(Cp)_2PF_6]$ as the oxidant, ~0.050 g of the insoluble polymer was suspended in 2 mL of toluene and the requisite amount of solid oxidant was added to the slurry. Although oxidant uptake was quite rapid as indicated by the almost immediate reduction of the ferricinium ion to ferrocene (monitored spectrophotometrically), the slurry was stirred overnight to promote uniform doping. The doped polymers were collected on a fritted disk, washed with copious amounts of toluene and hexanes to remove ferrocene, and dried for 30 min under a nitrogen flow. On the basis of porphyrin content and stoichiometric oxidant uptake, yields were typically

(15) (a) Collman, J. P.; Barnes, C. E.; Sweptson, P. N.; Ibers, J. A. *J. Am. Chem. Soc.* **1984**, *106*, 3500–3510. (b) Collman, J. P.; Barnes, C. E.; Woo, L. K. *Proc. Natl. Acad. Sci. U.s.A.* **1983**, *80*, 7684–7688.

(16) Collman, J. P.; Prodolliet, J. W.; Leidner, C. R. *J. Am. Chem. Soc.* **1986**, *108*, 2916–2921.

(17) Collman, J. P.; Brothers, P. J.; McElwee-White, L.; Rose, E.; Wright, L. J. *J. Am. Chem. Soc.* **1985**, *107*, 4570–4571.

(18) (a) Creutz, C.; Taube, H. *J. Am. Chem. Soc.* **1969**, *91*, 3988–3989. (b) Creutz, C. *Prog. Inorg. Chem.* **1983**, *30*, 1–73. (c) Kameke, A.; Tom, G.; Taube, H. *Inorg. Chem.* **1978**, *17*, 1790–1796.

(19) (a) Collman, J. P.; McDevitt, J. T.; Yee, G. T.; Leidner, C. R.; McCullough, L. G.; Little, W. A.; Torrance, J. B. *Proc. Natl. Acad. Sci. U.S.A.* **1986**, *83*, 4581–4585. (b) Collman, J. P.; McDevitt, J. T.; Yee, G. T.; Zisk, M. B.; Torrance, J. B.; Little, W. A. *Synth. Metals*, **1986**, *15*, 129–140.

(20) Perrin, D. D.; Armarego, W. L. F.; Perrin, D. R. *Purification of Laboratory Chemicals*; Pergamon: Oxford, 1980.

in the range 90–95%. In all cases, fluorine elemental analyses confirmed the expected stoichiometries.

**Optical Measurements.** All spectroscopic studies of the neutral and doped polymers were performed on samples dispersed in fluorolube mulls that were prepared in an inert-atmosphere box and placed between NaCl disks with 0.005-cm spacers. When it was necessary to normalize spectra to the same effective concentration, the porphyrin content was measured both by weighing the sample and the mulling agent and by using the C–H absorptions of the porphyrin as an internal spectroscopic standard. Spectra in the visible and near IR, 350–3000 nm, were recorded on a Beckman 5270 UV spectrophotometer.

Infrared measurements over the range 6000 to 1330 $cm^{-1}$ were recorded on an IBM FTIR 98 vacuum bench spectrophotometer using a globar source, KBr beam splitter, and HgCdTe and DTGS (deuteriated triglycine sulfate) detectors. The spectra were obtained at 1 $cm^{-1}$ resolution with a zero filling of four, averaging the data of 128 scans. After the interferograms were transformed and a ratio to the background spectrum (neat Fluorolube/NaCl) was obtained, the spectra were converted to absorbance units. In the spectral windows described above, Fluorolube was found to be free of any appreciable absorbance; hence the data reported herein reflect the intrinsic spectral properties of the polymers without interference from the mulling agent.

**Pressed Powder Conductivity Measurements.** Sample disks (7-mm diameter and approximately 1 mm thick) were prepared by compacting powders with a hand-held pellet press in a glovebox. Disk thickness was determined with a micrometer. Standard linear four-point probe measurements on the pressed powders of the more conductive samples were obtained by using an Allessi Industries (Costa Mesa, CA) probe head (pin spacing 1.0 mm) connected to a Keithly (Cleveland, OH) 220 programmable current source and a Keithly 610C electrometer. Standard two-point probe measurements were made on the more resistive samples by using the same electronics. Two 7-mm polished stainless-steel dies, a Teflon collar, and a press were employed to make these measurements. Resistivities were calculated by using standard equations.[21]

**Electrochemistry.** All experiments were performed in the glovebox by using standard three electrode cells and instrumentation. Potentials were measured vs. the Ag/AgCl pseudo-reference electrode and converted to SSCE (SSCE = sodium chloride saturated calomel electrode) by using ferrocene as an external standard.

**Carbon Paste Electrodes.** Carbon paste[22] was prepared by mulling 1–10 mg of sample, 50 mg of graphite powder, 21 mg of sodium dodecylsulfate, and 32 mg of Nujol until a smooth paste resulted. The paste was compacted into a depression (0.5-cm diameter, 0.2 cm deep) in a Teflon rod and smoothed by gentle polishing on a piece of weighing paper. Electrical contact was made to the paste through a Pt wire at the bottom of the depression.

**Carbon Cloth Electrodes.** Pieces of graphite cloth ~1 $cm^2$ (GC14, Electrosynthesis Co., East Amherst, NY) were impregnated with 1–3 mg of polymer by gently rubbing the solid into the cloth using a spatula. The cloth was picked up with forceps and gently shaken to remove any loosely adhering solid. For selected samples the carbon cloth was weighed before and after loading the polymer to provide a measure of the sample used.

**Cyclic Voltammetry Experiments.** The cyclic voltammetric response of the polymers in carbon paste and at carbon cloth were measured in $CH_3CN$ containing 0.1 M $Et_4NX$, where X = $ClO_4^-$, $BF_4^-$, or $PF_6^-$. Scan rates of 1–10 mV/s were typically employed in these studies. Because many of the waves were unsymmetric, thermodynamic potentials could only be approximated. The formal potentials reported throughout this paper, $E_0'$, are taken to be the average of the anodic and cathodic peak potentials [$E_0' = (E_{pa} + E_{pc})/2$].

**Potential Step Experiments.** The electrochemical cell was assembled with the polymer-loaded carbon cloth and the potentiostat at open circuit. The current flowing through the cell was monitored with the recorder on time base as the cell was connected to the "initial" potential. Potential steps could then be performed to assay the amount of charge necessary to oxidize or reduce the polymer completely to the redox state dictated by the applied potential (the background currents of the bare graphite cloth were insignificant compared to the Faradaic currents).

## Results and Discussion

**Synthesis and Characterization.** As illustrated by eq 4, the metalloporphyrin dimers $[Ru(OEP)]_2$ and $[Os(OEP)]_2$ react with a variety of bridging ligands—pyrazine (pyz), 4,4′-bipyridine (bpy), and 1,4-diazabicyclo[2.2.2]octane (dabco)—to produce

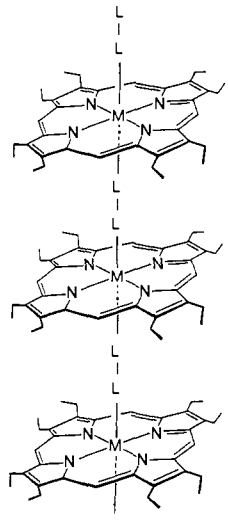

Figure 1. Proposed structure of the octaethylporphyrin coordination polymers where M = {Fe, Ru, Os} and L-L = {pyrazine, 4,4′-bipyridine, dabco}.

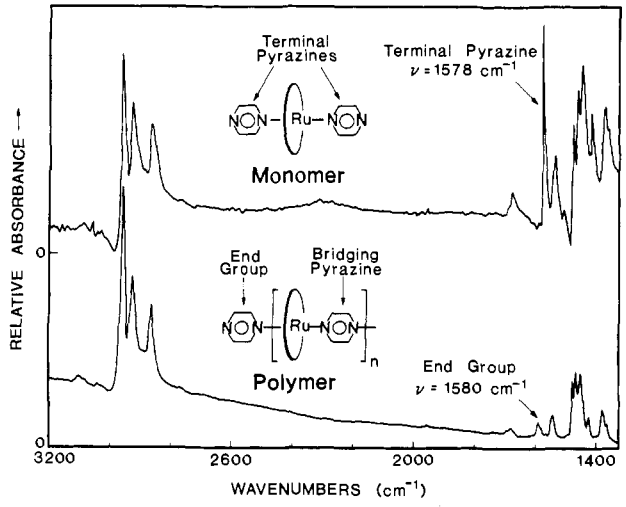


Figure 2. Infrared absorbance spectra of $Ru(OEP)(pyz)_2$ and $[Ru(OEP)(pyz)]_n$ illustrating the presence of the pyrazine breathing mode at 1578 $cm^{-1}$ for the former complex and the near absence of this mode in the spectrum of the polymer. Specta have been normalized to the same porphyrin content and have been offset along the $y$ axis for clarity.

polymeric structures of the type shown in Figure 1. In general, the dimers are dissolved in toluene, and 1 equiv (M/L-L = 1.00) of the bridging ligand is added to the solution. The soluble starting materials are converted to insoluble powders leaving the solution virtually colorless. Although the analysis of the powders is hampered by their insolubility in noncoordinating solvents, each has yielded satisfactory C, H, N elemental analyses and has been studied by infrared spectroscopy, the results of which are consistent with the proposed polymeric structure (vide infra).

We have observed that the rate at which these materials polymerize varies considerably, depending on both the metal, in the order Fe > Ru > Os, and the ligand with dabco > bpy > pyz. Because the polymerization rate affects the chain length, we used the reaction temperature, the choice of solvent, and the reaction time to control polymer growth so as to obtain materials of similar chain length.

**End Group Analysis.** The colligative properties of polymer solutions are usually employed to measure molecular weights. However, since the present materials are virtually insoluble, an alternative spectroscopic method was employed. This method relies on the infrared absorption bands of the bridging ligands that depend on their local symmetry.[23] Pyrazine and 4,4′-bipyridine[24]

(21) Sze, S. M. *Physics of Semiconductor Devices*; Wiley: New York, 1981; pp 30–35.
(22) Marcoux, L. S.; Prater, K. B.; Prater, B. G.; Adams, R. N. *Anal. Chem.* **1965**, *37*, 1446–1447.

exhibit a characteristic centrosymmetric ring stretching mode near 1600 $cm^{-1}$ which is infrared and Raman active for the unidentate ligands and infrared silent and Raman active for bidentate and free ligand. Figure 2 illustrates these features for $[Ru(OEP)(pyz)]_n$ and $Ru(OEP)(pyz)_2$. The spectrum of the monomer exhibits a strong absorption at 1578 $cm^{-1}$ as expected for unidentate pyrazine. The spectrum of the polymer, normalized to the same porphyrin content, displays a dramatic decrease in intensity and a slight shift in the frequency of this band; this behavior is consistent with a high proportion of symmetrically bridging pyrazine. Similar behavior is found with the iron and osmium congeners.[19b] The small residual absorption in the spectra of the polymers near 1580 $cm^{-1}$ arises from the presence of unidentate pyrazines that cap the ends of the polymer chains.

This type of end group analysis has been utilized previously to estimate the chain length of similar pyrazine and 4,4′-bipyridine-bridged polymers.[23b,c] However, many of those studies were plagued by uncertainties concerning assignments and problems with interfering absorbances. In order to overcome these problems, we synthesized and analyzed the infrared spectra of the bis(pyrazine-$d_4$) monomers and $\mu$-pyrazine-$d_4$ polymers of Ru(OEP) and Os(OEP). Table I summarizes the results from this study. Comparison of these data with the published porphyrin[25] and pyrazine literature[23a,b] has permitted the assignment of most of the absorptions in the spectral range 4000–1330 $cm^{-1}$. Because of the complex and highly coupled nature of these modes, it is impossible to assign simple isolated modes to each of the bands in the spectra. However, with the isotopic substitution, it was possible to determine whether a particular band was predominantly porphyrin or predominantly pyrazine based. Further classification of specific modes were made in a more tentative fashion in accordance with the original porphyrin and pyrazine conventions.[23,25]

With this analysis, the extent of polymerization was determined from the ratio of the absorbance of the pyrazine $\nu_{8a}$ mode of the bis(pyrazine) monomer to that of the $\mu$-pyrazine polymer, normalized to the same porphyrin content.[26] Typical values for the chain length of the $[M(OEP)(pyz)]_n$ polymeric series are $n = 40$ ($\pm$ 10) for iron, $n = 25$ ($\pm$ 5) for ruthenium, and $n = 20$ ($\pm$ 5) for osmium.

**Doping Reactions.** The coordination polymers described here can be oxidized with a nonstoichiometric amount of oxidant, $\rho$ ($\rho$ is the oxidant mole fraction), where $0 < \rho < 1$, to produce highly conductive solids (eq 5). Concurrent with the polymer oxidation

$$[M^{2+}(OEP)(L\text{-}L)] + \rho[ox] \rightarrow [M^{2+}_{1-\rho}M^{3+}_{\rho}(OEP)(L\text{-}L)](A^-)_\rho \quad (5)$$

is the incorporation of an anion, $A^-$, which serves to maintain charge neutrality. A variety of oxidants [iodine ($I_2$), nitrosyl hexafluorophosphate ($NOPF_6$), ferricinium hexafluorophosphate ($FeCp_2PF_6$), molecular oxygen ($O_2$)] can be employed as dopants; in most cases, complete reaction of the oxidant occurs almost immediately. The coordination properties of the dopant anion and the redox potential of the dopant[19b] are important considerations in choosing the oxidant for the doping reaction. Listed below are the half-cell reactions of the oxidants employed in our doping studies.[28] The gaseous NO evolved in eq 6 was removed completely by vacuum as verified by the absence of coordinated NO bands in the infrared spectra. Ferrocene formed in eq 7 was

$$e^- + NOPF_6 \rightarrow NO + PF_6^- \quad E_0' = 1.27 \text{ V vs. SSCE} \quad (6)$$

$$e^- + FeCp_2PF_6 \rightarrow FeCp_2 + PF_6^- \quad E_0' = 0.39 \text{ V vs. SSCE} \quad (7)$$

$$e^- + {}^3/_2I_2 \rightarrow I_3^- \quad E_0' = 0.63 \text{ V vs. SSCE} \quad (8)$$

$$e^- + {}^x/_2I_2 \rightarrow I_x^- \quad (9)$$

**Table I**

A. Vibrational Frequencies ($cm^{-1}$) and Assignments for Pyrazine Monomers and Polymers of Ru(OEP)

| Ru(OEP)-(pyz)$_2$ | Ru(OEP)-(pyz-$d_4$)$_2$ | [Ru(OEP)-(pyz)]$_n$ | [Ru(OEP)-(pyz-$d_4$)]$_n$ | assignt |
|---|---|---|---|---|
| 2958 (vs) | 2962 (vs) | 2961 (vs) | 2962 (vs) | $\nu_{aCH_3}$(C–H) OEP |
| 2926 (s) | 2929 (s) | 2929 (s) | 2929 (s) | $\nu_{aCH_2}$(C–H) OEP |
| 2865 (s) | 2868 (s) | 2867 (s) | 2868 (s) | $\nu_{sCH_2,CH_3}$(C–H) OEP |
| 1681 (w) | 1682 (w) | 1679 (w) | 1681 (w) | $\nu_{C=C}$ OEP |
| 1590 (vw) | 1592 (w) | 1589 (w) | 1593 (w) | $\nu_{C=N}$ OEP |
| 1578 (s) | 1534 (s) | 1580 (sh, w) | | ring 8a pyz |
| 1539 (m) | 1538 (sh, m) | 1543 (m) | 1543 (w) | OEP |
| 1510 (vw) | 1487 (w) | | | ring 8b pyz |
| 1477 (m) | 1370 (sh) | 1478 (m) | 1375 (w)[a] | ring 19a pyz |
| 1464 (ms) | 1464 (ms) | 1466 (ms) | 1466 (ms) | $\nu_{C=N}$, $\delta_{CCN}$ OEP |
| 1449 (ms) | 1452 (ms) | 1450 (ms) | 1450 (ms) | $\delta_{CH}$, $\delta_{CH_3}$ OEP |
| 1418 (m) | 1175[b] | 1425 (m) | 1175[b] | ring 19b pyz |
| 1377 (m) | 1378 (m) | 1379 (m) | 1379 (m) | $\delta_{CH_3}$ OEP |
| 1372 (m) | 1368 (w) | 1370 (sh) | 1375 (w)[a] | OEP |
| 1362 (w) | 1362 (w) | 1363 (w) | 1365 (w) | OEP |
| | 1338 (w) | | | pyz |

B. Vibrational Frequencies ($cm^{-1}$) and Assignments for Pyrazine Monomers and Polymers of Os(OEP)

| Os(OEP)-(pyz)$_2$ | Os(OEP)-(pyz-$d_4$)$_2$ | [Os(OEP)-(pyz)]$_n$ | [Os(OEP)-(pyz-$d_4$)]$_n$ | assignt |
|---|---|---|---|---|
| 2963 (s) | 2959 (s) | 2961 (vs) | 2957 (vs) | $\nu_{aCH_3}$(C–H) OEP |
| 2929 (s) | 2929 (s) | 2929 (m) | 2925 (s) | $\nu_{aCH_2}$(C–H) OEP |
| 2865 (ms) | 2864 (ms) | 2867 (m) | 2860 (s) | $\nu_{sCH_2,CH_3}$(C–H) OEP |
| 1680 (vw) | 1682 (vw) | 1681 (vw) | 1679 (w) | $\nu_{C=C}$ OEP |
| 1592 (vw) | | 1590 (sh, w) | 1591 (w) | $\nu_{C=N}$ OEP |
| 1568 (vvs) | 1526 (vvs) | 1578 (w) | 1533 (w) | Ring 8a pyz |
| 1547 (m) | 1547 (m) | 1546 (m) | 1545 (sh) | OEP |
| 1496 (m) | 1476 (m) | | | ring 8b pyz |
| 1475 (m) | 1370 (sh) | 1470 (s)[a] | 1373 (m)[a] | Ring 19a pyz |
| 1468 (mw) | 1468 (m) | 1470 (s)[a] | 1465 (m) | $\nu_{C=N}$, $\delta_{CCN}$ OEP |
| 1452 (m) | 1453 (m) | 1449 (m) | 1447 (m) | $\delta_{CH_2,CH_3}$ OEP |
| 1442 (mw) | 1443 (m) | 1445 (sh) | 1440 (sh) | OEP |
| 1415 (s) | 1175[b] | 1435 (m) | 1175[b] | ring 19b pyz |
| 1378 (m) | 1378 (m) | 1382 (mw) | 1380 (m) | $\delta_{CH_3}$ OEP |
| 1367 (m) | 1367 (m) | 1375 (mw) | 1373 (m)[a] | OEP |
| 1362 (m) | 1362 (m) | 1365 (m) | 1364 (m) | OEP |
| | 1331 (m) | | | pyz |

[a] Dual assignment due to band overlap. [b] Band occurs at a frequency outside the acquired spectral window. Reported frequency based on literature values.

(23) (a) Simmons, J. D.; Innes, K. K. *J. Mol. Spectrosc.* **1964**, *14*, 190–197. (b) Metz, J.; Schneider, O.; Hanack, M. *Spectrochim. Acta, Part A* **1982**, *38A*, 1265–1273 and references therein. (c) Lord, R. C.; Marston, A. L.; Miller, F. A. *Spectrochim. Acta* **1957**, *9*, 113–125.

(24) (a) Bidentate 4,4′-bipyridine is centrosymmetric with respect to the 4,4′-bond center if both pyridyl units are coplanar as was the case $[Co(dmgH)_2(bpy)]_n$ (see ref 24b). (b) Strähle, J.; Kubel, F.; Hiller, W.; Dantona, R. *Mol. Cryst. Liq. Cryst.* **1982**, *81*, 265–272.

(25) (a) Ogoshi, H.; Masai, N.; Yoshida, Z.; Takemoto, J.; Nakamoto, K. *Bull. Chem. Soc. Jpn.* **1971**, *44*, 49–51. (b) Alben, J. O. In *The Porphyrins, Physical Chemistry Part A*; Dolphin, D., Ed.; Academic: New York, 1978; Vol. III, Chapter 7. (c) Ogoshi, H.; Saito, Y.; Nakamoto, K. *J. Chem. Phys.* **1972**, *57*, 4194–4202.

(26) For this end group analysis we assumed, as did the previous authors who employed this method, that all the polymer chains were fully capped. We believe this assumption is valid in view of the fact that group VII transition-metal porphyrins normally display a high affinity for two axial ligands.[27]

(27) Buchler, J. W. In *The Porphyrins, Structure and Synthesis Part A*; Dolphin, D., Ed.; Academic: New York, 1978; Vol. I, pp 447–468.

(28) Formal potentials, $E_0'$, shown in eq 6–8 were obtained by cyclic voltammetry for solutions of the oxidants; 0.1 M $Et_4NClO_4/CH_3CN$ for ferrocene and iodine and 0.2 M $Bu_4NClO_4/CH_2Cl_2$ for nitrosyl hexafluorophosphate. Although the first two oxidants were well behaved electrochemically, $NO^+/NO$ displayed only a quasi-reversible wave. The $E_0'$ value reported here was determined according to $E_0' = (E_{pa} + E_{pc})/2$. The $E_0'$ values for $I_2/I_5^-$, $I_2/I_7^-$, etc. (eq 9) were not examined in this study and therefore have not been reported here.

Table II. Room-Temperature Pressed Powder Conductivities

| compound | oxidant | $\rho$ | $\sigma_{RT}$, $(\Omega\ cm)^{-1}$ |
|---|---|---|---|
| $Fe(OEP)(pyz)_2$ | | | $2.8 \times 10^{-11}$ [a] |
| $[Fe(OEP)(pyz)]_n$ | | | $1.1 \times 10^{-10}$ [a] |
| $[Fe(OEP)(pyz)(PF_6)_\rho]_n$ | $FeCp_2PF_6$ | 1/3 | $2.1 \times 10^{-5}$ [b] |
| $[Fe(OEP)(pyz)I_\rho]_n$ | $I_2$ | 1.0 | $3.0 \times 10^{-11}$ [a,b] |
| $Ru(OEP)(pyz)_2$ | | | $1.0 \times 10^{-11}$ [a] |
| $[Ru(OEP)(pyz)]_n$ | | | $1.2 \times 10^{-8}$ [a,b] |
| $[Ru(OEP)(pyz)I_\rho]_n$ | $I_2$ | 2/3 | $1.4 \times 10^{-2}$ [b] |
| $[Ru(OEP)(pyz)(PF_6)_\rho]_n$ | $NOPF_6$ | 2/3 | $3.0 \times 10^{-3}$ [b] |
| $[Ru(OEP)(bpy)]_n$ | | | $1.6 \times 10^{-9}$ [a,b] |
| $[Ru(OEP)(bpy)(PF_6)_\rho]_n$ | $FeCp_2PF_6$ | 1/3 | $3.0 \times 10^{-4}$ [b] |
| $[Ru(OEP)(dabco)]_n$ | | | $2.5 \times 10^{-10}$ [a,b] |
| $[Ru(OEP)(dabco)(PF_6)_\rho]_n$ | $FeCp_2PF_6$ | 1/3 | $2.6 \times 10^{-6}$ [b] |
| $Os(OEP)(pyz)_2$ | | | $8.0 \times 10^{-11}$ [a] |
| $[Os(OEP)(pyz)]_n$ | | | $3.2 \times 10^{-7}$ [a,b] |
| $Os(OEP)(pyz)I_\rho]_n$ | $I_2$ | 1.0 | $1.5 \times 10^{-2}$ [b] |
| $[Os(OEP)(pyz)(PF_6)_\rho]_n$ | $FeCp_2PF_6$ | 1/5 | $2.3 \times 10^{-2}$ [b] |
| $[Os(OEP)(bpy)]_n$ | | | $1.0 \times 10^{-8}$ [a,b] |
| $[Os(OEP)(bipy)(PF_6)_\rho]_n$ | $FeCp_2PF_6$ | 1/3 | $2.6 \times 10^{-3}$ [b] |
| $[Os(OEP)(dabco)]_n$ | | | $3.2 \times 10^{-8}$ [a,b] |
| $[Os(OEP)(dabco)(PF_6)_\rho]_n$ | $FeCp_2PF_6$ | 1/3 | $1.2 \times 10^{-6}$ [b] |

[a] Two-point probe measurement made under pressure. [b] Standard linear four-point probe measurement.

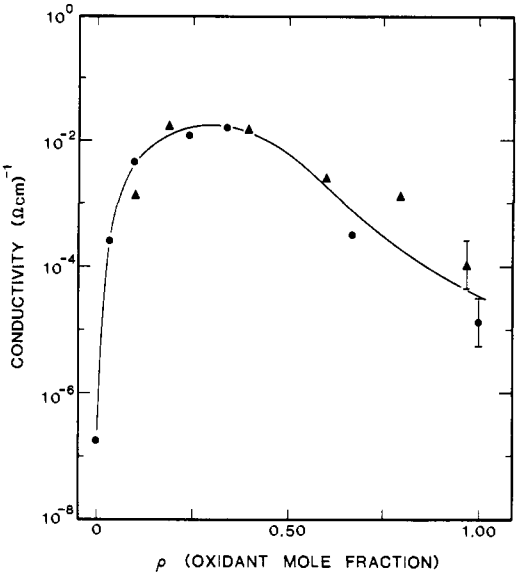


Figure 3. Plot of the room-temperature pressed powder conductivity values for $[Os(OEP)(pyz)]_n$ as a function of $\rho$, where $\rho$ is the fraction of oxidized oxmium centers within the polymer. Data are shown for both (▲) ferricinium hexafluorophosphate and (●) iodine-doped systems.

washed away with toluene and hexanes. For these two oxidants, C, H, N, and F elemental analyses confirm the reaction stoichiometry; the degree of oxidation, $\rho$, can be calculated directly from these determinations. Such is not the case when iodine is employed as the oxidant because of the many possible forms of polyiodide anion. Resonance Raman spectra of $[Os(OEP)(pyz)I_{1.0}]$ reveal that $I_3^-$ is the predominant form of iodine. Further studies are necessary to determine the form of the polyiodide anions at other dopant levels and in other polymer systems.

**Conductivity Studies.** Room-temperature conductivities of the neutral and doped coordination polymers of octaethylporphyrin bridged with dabco, bpy, and pyz are provided in Table II. Values for bis(pyrazine) monomers have been provided for comparison. These conductivity values were determined anaerobically on compacted pressed powders. By their nature, these measurements are influenced by interparticle and interchain contact resistance and are averaged over all crystallographic orientations. Pressed powder conductivity values are typically 2–3 orders of magnitude less than their single-crystal counterparts.[29]

Conductivity values of the bis(pyrazine) complexes fall into the range expected for undoped monomeric porphyrins: $10^{-10}$–$10^{-11}$ $\Omega^{-1}$ cm$^{-1}$.[30] All the polymers show a significant increase in conductivity relative to their respective monomers with a trend toward higher conductivity as the iron triad is descended. However, this trend may be the result of adventitious oxygen doping. In fact, $[Os(OEP)(pyz)]_n$ displays a $10^3$ increase in conductivity following only a brief exposure to oxygen. Such behavior may be responsible for the remarkably high conductivities of many of the "undoped" polymers of this type that have been reported previously in the literature.[31]

Because the effects of adventitious doping are no longer significant after moderate doping has occurred, we may more easily evaluate the trends exhibited by the conductivities of the doped polymers. Inspection of Table II reveals increasing conductivity for the doped samples both as the iron triad is descended and with respect to the bridging ligand in the order dabco < bpy < pyz. We believe these trends are the result of the differing ability of the three bridging ligands to mediate electron exchange between the metal(II) and metal(III) sites along the chain. The important interaction in this regard is the mixing of the metal's $d_\pi$ ($d_{xz}$, $d_{yz}$) with the $\pi^*$ level of the bridging ligand. Thus the metal–metal communication is greater for the better $\pi$-bonding metals—Os > Ru > Fe—and through the more $\pi$-acidic bridging ligand—pyz > bpy ≫ dabco.

The oxidant mole fraction was also found to have a dramatic effect on the conductivity. Figure 3 illustrates the dependence of the conductivity of $[Os(OEP)(pyz)]_n$ on $I_2$ and $FeCp_2PF_6$ oxidant mole fraction. For the purpose of this figure, we have assumed that within the polymer matrix all the iodine exists in the form of $I_3^-$. Like most conductive polymers, the initial small degree of oxidation produces the most dramatic increase in the conductivity. However, unlike polyacetylene,[32] $[M(Pc)FI_x]_n$ (M = Al, Ga, Cr),[12c,d] $[M(Pc)OI_x]_n$ (M = Si, Ge),[33] and $[M(OEP)I_x]$ (M = $H_2$, Cu, Zn),[34] where the conductivity increases monotonically with doping and levels off only at the highest obtainable dopant mole fraction, $[Os(OEP)(pyz)]_n$ reaches a conductivity maximum at $\rho$ = 0.2–0.4 and then falls off at higher oxidant mole fractions. We have obtained similar results with $[Ru(OEP)(pyz)]_n$. This type of behavior also has been observed recently with doped polyaniline systems[35] and oxo-bridged silicon phthalocyanine.[36]

**Electrochemistry.** Electrochemical methods have been employed in the preparation, doping, and characterization of many conductive polymers and molecular metals. As noted earlier, the oxidative doping of the $[M(OEP)(L\text{-}L)]_n$ polymers results in dramatic increases in conductivity. The identification of the site of these oxidations provides insight into the conduction pathway. Although ESR studies of low dimensional conductors have often been employed to address such an issue, many of these studies have been found to be unreliable. At certain dopant levels, polyacetylene,[37] polyparaphenylene,[38] and polypyrrole[39] display conductivities that are not associated with unpaired electrons but rather with spinless charge carriers. The absence of vibrational

(29) Coleman, L. *Rev. Sci. Instrum.* **1978**, *49*, 58–62.
(30) Gutman, F.; Lyons, L. *Organic Semiconductors*; Wiley: New York, 1967.
(31) (a) Metz, J.; Hanack, M. *J. Am. Chem. Soc.* **1983**, *105*, 828–830. (b) Datz, A.; Schneider, O.; Hanack, M. *Synth. Met.* **1984**, *9*, 31–40. (c) Schneider, O.; Hanack, M. *Angew. Chem., Int. Ed. Engl.* **1983**, *22*, 784–785.
(32) Chiang, C. K.; Heeger, A. J.; MacDiarmid, A. G. *Ber. Bunsenges. Phys. Chem.* **1979**, *83*, 407.
(33) Diel, B. N.; Inabe, T.; Lyding, J. W.; Schock, K. F., Jr.; Kannewurf, C. R.; Marks, T. J. *J. Am. Chem. Soc.* **1983**, *105*, 1551–1567.
(34) Wright, S. K.; Schramm, C. J.; Phillips, T. E.; Scholler, D. M.; Hoffman, B. M. *Synth. Met.* **1979**, *1*, 43–51.
(35) McManus, P. M.; Yang, S. C.; Cushman, R. J. *J. Chem. Soc., Chem. Commun.* **1985**, *22*, 1556–1557.
(36) Gaudiello, J. G.; Marcy, H. O.; McCarthy, W. J.; Moguel, M. K.; Kannewurt, C. R.; Marks, T. J. *Synth. Met.* **1986**, *15*, 115–128.
(37) Ikehata, S.; Kaufer, J.; Woerner, T.; Pron, A.; Druy, M. A.; Sivak, A.; Heeger, A. J.; MacDiarmid, A. G. *Phys. Rev. Lett.* **1980**, *45*, 1123–1126.
(38) Peo, M.; Roth, S.; Dransfeld, K.; Tieke, B.; Hocker, J.; Gross, H.; Grupp, A.; Sixl, H. *Solid State Commun.* **1980**, *35*, 119–122.
(39) Scott, J. C.; Krounbi, M.; Pfluger, P.; Street, G. B. *Phys. Rev. B: Condens. Matter* **1983**, *28*, 2140–2145.

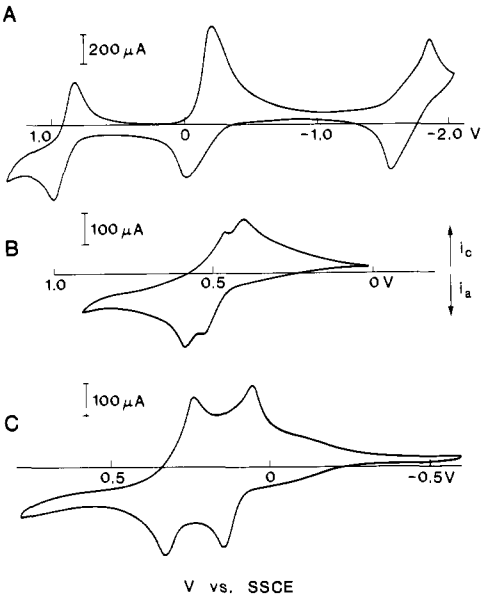


**Figure 4.** Cyclic voltammetric response in 0.1 M $Et_4NClO_4/CH_3CN$ recorded at carbon cloth electrodes of (A) $[Os(OEP)(bpy)]_n$ (5 mV/s), (B) $[Ru(OEP)(pyz)]_n$ (2 mV/s), and (C) $[Os(OEP)(pyz)]_n$ (2 mV/s).

bands in the IR characteristic of porphyrin $\pi$-radical cations in our doped polymers provides indirect evidence that the doping is metal-centered and the conduction pathway is through the metal spine, but more direct evidence was desired. We were able to obtain such information by examining the electrochemical properties of our polymers. In addition, these studies provided useful information for the selection of dopants.

The insolubility of these polymers precludes solution electrochemistry, and the method of their preparation makes film electrochemical methods difficult. The electrochemical properties of intractable materials have often been explored by a carbon paste technique.[22] We examined our polymers with this method and found the results to be unsatisfactory. The electrochemical responses of our polymers were not quantitatively reproduced from sample to sample and suffered from the limited range (−0.6 to 1.2 V vs. SSCE in 0.1 M $Et_4NClO_4/CH_3CN$) characteristic of carbon paste.[22] We were able to obtain satisfactory results, however, employing carbon cloth as the electrode support material. Carbon cloth electrodes have been used previously, mainly in industrial laboratories for battery research and catalytic applications where high surface area and chemically inert electrode materials are required, but we are unaware of previous studies of conductive polymer systems employing this technique. The results obtained with the carbon cloth electrodes were in good qualitative agreement with the carbon paste electrodes for all the polymers studied; however, the cloth electrodes provided more reproducible and quantitative results as well as more highly reversible looking waves than did the paste electrodes. We feel that in the future, electrochemists are likely to adopt this method in preference to the more established paste technique. For the purpose of this paper only the results obtained with the cloth electrodes will be discussed.

The cyclic voltammetric response of a carbon cloth impregnated with $[Os(OEP)(bpy)]_n$ in 0.1 M $Et_4NClO_4/CH_3CN$ is depicted in Figure 4A. This polymer, as well as the others described herein, can be cycled repeatedly between its neutral and oxidized forms without change in its overall electrochemical responses, demonstrating the chemical reversibility of this process. However, as with many of the previous electrochemical studies of conductive polymers, ideal cyclic voltammetry response for the surface-confined species are not observed. The shape of the cyclic voltammogram is strongly dependent on the scan rate. At high scan rates (≥20 mV/s), the fine structure of the waves (multiple wave characteristics, vide infra) is lost and the waves are broad and ill-defined; this behavior probably results from a combination of slow charge transport and resistance problems within the polymer film. At scan rates such as those employed in Figure 4A (5 mV/s), well-defined, reproducible cyclic voltammetric waves are readily obtained. Attempts were made to correlate the amount of electroactive material with that applied to the electrode, but a noticeable amount of the solid was dislodged from the carbon cloth upon addition of solvent to the cell. In the experiment depicted in Figure 4A, ~70% of the material applied to the carbon cloth is electrochemically detected; the remainder of the applied material is presumably accounted for by that suspended in solution. For this sample and all of those described in this report it is assumed that all of the material on the cloth is electroactive.

**Table III.** Summary of Electrochemical Data[a]

| compound | $E_0'$ ($M^{2+/3+}$) | $\Delta E_{ox}$.[b] | $E_0'$- ($OEP^{0/+}$) | $E_0'$- ($OEP^{0/-}$) |
|---|---|---|---|---|
| $[Ru(OEP)(dabco)]_n$ | 0.09 | 0 | | |
| $[Os(OEP)(dabco)]_n$ | 0.11 | 0 | | |
| $[Ru(OEP)(bpy)]_n$ | 0.24, 0.28 | 0.035 | 1.11 | −1.75 |
| $[Os(OEP)(bpy)]_n$ | −0.08, −0.12 | 0.044 | 0.94 | −1.67 |
| $[Fe(OEP)(pyz)]_n$ | 0.35 | 0 | | |
| $[Ru(OEP)(pyz)]_n$ | 0.50, 0.55 | 0.050 | | |
| $[Os(OEP)(pyz)]_n$ | 0.15, 0.33 | 0.185 | 1.03 | −1.59 |

[a] All electrochemical studies were performed in 0.1 M $Et_4NClO_4/CH_3CN$ at carbon cloth electrodes. Potentials are reported relative to SSCE. [b] $\Delta E$ is a measure of the splitting observed for the metal-based waves and is reported in volts.

The cyclic −1.67 V voltammogram of $[Os(OEP)(bpy)]_n$ displays three waves at 0.94, −0.10, and −1.67 V vs. SSCE. Potential step experiments (vide infra) were performed on this material to determine that the couples at 0.94 and −0.10 V represent oxidations and the couple at −1.67 V represents a reduction. By comparison with the $Ru(OEP)(py)_2$ and $Os(OEP)(py)_2$ monomers,[40] these waves are attributed to the $OEP^{0/+}$, Os(II/III), and $OEP^{0/-}$ couples, respectively. Likewise, most metalloporphyrin complexes display ring oxidations near 1 V vs. SSCE.[40b] The presence of oxidative couples at considerably less positive potentials than this value for the other neutral polymers (Table III) indicates that the transition-metal sites are more readily oxidized than the porphyrin ligands in these polymers. This implies that if the oxidation stoichiometry is controlled ($0 < \rho < 1$), the doping of the polymers described here should occur at the metal, not at the porphyrin.

The cyclic voltammetric response of the $[Ru(OEP)(pyz)]_n$ and $[Os(OEP)(pyz)]_n$ polymers on carbon cloth electrodes, parts B and 4C, respectively, of Figure 4, exhibits an interesting phenomenon. At low scan rates the metal-centered redox waves centered at 0.53 V for the Ru polymer and 0.24 V for the Os polymer are resolved into two closely spaced waves. Such splitting of the metal-centered waves is also observed in other polymers described herein. Table III contains a measure of this splitting, designated $\Delta E_{ox}$. Potential step experiments were employed to determine the nature of these metal-centered waves and to determine the number of electrons involved in each couple. In the potential step experiments, a small amount of each polymer was loaded onto a carbon cloth electrode at open circuit. The potential of the electrode was then stepped to either side of the waves observed in the cyclic voltammetric studies, and the current vs. time response was recorded. Parts A and B of Figure 5 are the traces for the neutral polymer $[Os(OEP)(pyz)]_n$ recorded at −0.3 and 0.7 V vs. SSCE, respectively. Whereas very little current response was recorded when the neutral polymer was exposed to the initial reducing potential, a large current flow was observed when the sample was stepped to the oxidizing potential. Parts C and D of Figure 5 illustrate the traces for the chemically oxidized polymer, $[Os(OEP)(pyz)(PF_6)_{1.0}]_n$. At the oxidizing potentials, only a small current was observed;[41] however, when

(40) (a) Brown, G. M.; Hopf, F. R.; Ferguson, J. A.; Meyer, T. J.; Whitten, D. G. *J. Am. Chem. Soc.* **1973**, *95*, 5939–5942. (b) Felton, R. H. In *The Porphyrins*; Dolphin, D., Ed.; Academic: New York, 1978; Vol. V., pp 53–125.

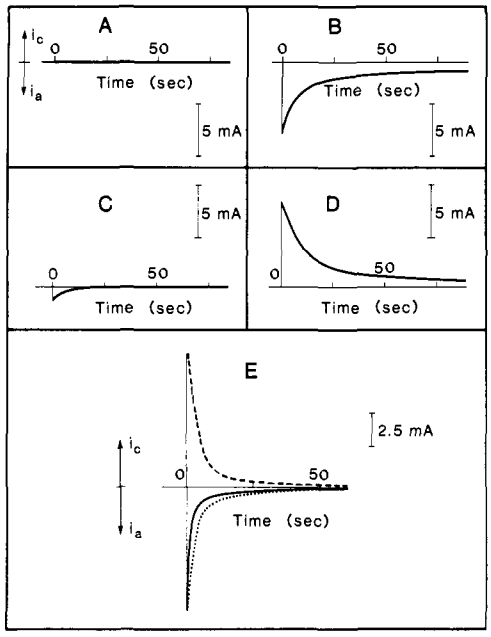


Figure 5. Potential step traces for undoped and chemically oxidized samples of $[Os(OEP)(pyz)]_n$ confined to a carbon cloth electrode in 0.1 M $Et_4NClO_4/CH_3CN$. Current vs. time traces are recorded at the oxidizing potential of 0.7 V and the reducing potential of −0.3 V vs. SSCE. (A) and (B) represent traces recorded for a sample of $[Os(OEP)(pyz)]_n$ initially at the reducing potential (A) and then at the oxiding potential (B). (C) and (D) are traces recorded for $[Os(OEP)(pyz)(PF_6)_{1.0}]_n$ at the oxidizing (C) and then the reducing potential (D). (E) Current vs. time traces for a sample of $[Os(OEP)(pyz)(PF_6)_{0.4}]_n$ recorded first at the oxidizing potential (—), then at the reducing potential (---), and finally back to the oxidizing potential (···).

the potential was stepped back to the reducing potential, a large cathodic current flowed. These experiments confirm that both waves are oxidations. Figure 5E shows three potential step traces for $[Os(OEP)(pyz)(PF_6)_{0.4}]_n$ recorded sequentially on the same sample at potentials of 0.7, −0.3, and 0.7 V vs. SSCE. At the first potential, the remainder of the polymer not oxidized chemically was oxidized electrochemically. During the second excursion, the entire polymer was reduced back to its neutral state, and during the last trace, the entire polymer was reoxidized. Relative areas of 0.58, 1.00, and 0.96, respectively, were swept out in these traces. From the initial stoichiometry of the chemical oxidation and these relative areas it is apparent that the sum of the two waves represents a single electron oxidation of the repeating monomer unit. If each wave were associated with a one-electron process in itself, relative areas of 0.80, 1.00, and 1.00 would have been observed. Therefore, the first wave would seem to correspond to the oxidation of the polymer to an Os(II/III) mixed-valence state (half or approximately half oxidized polymer) and the second wave to the oxidation of the remainder of Os(II) sites. It is important to emphasize here that in using this technique, it is not necessary to know the precise amount of polymer that is electroactive in each experiment. It is the relative areas under the current vs. time traces and knowledge of the stoichiometry of the chemical doping that allows for an assessment of the number of electrons involved in each wave.

In addition to the polymers described in this paper, anomalous electrochemical responses of conductive polymers have been observed in studies of polyacetylene and polyphenylene.[42] In these

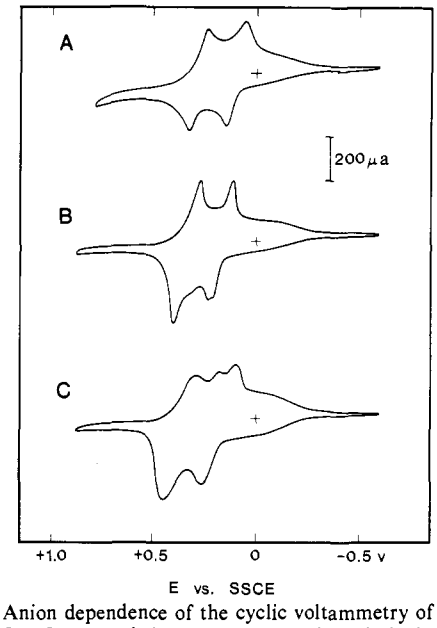


Figure 6. Anion dependence of the cyclic voltammetry of $[Os(OEP)(pyz)]_n$ in $CH_3CN$ recorded at 2 mV/s at carbon cloth electrodes with a 0.1 M supporting electrolyte of (A) $Et_4NClO_4$, (B) $Et_4NPF_6$, and (C) $Et_4NBF_4$.

systems, the electrochemical responses were accompanied by discrete structural phase changes. The identity of these crystallographic phases and their effect on the electrochemical response of the host polymer were found to be strongly dependent on the intercalated ion. In order to probe this effect in our polymers, the anion dependence was studied. The cyclic voltammetric responses of $[Os(OEP)(pyz)]_n$ in the presence of $ClO_4^-$, $BF_4^-$, and $PF_6^-$, shown in Figure 6, display a moderate anion effect and suggest that structural changes may be operative in this system also. Electrostatic screening and/or pinning of the conduction electrons by the dopant anions may also be important factors in explaining these results. Inspection of Table III reveals that the magnitude of the splitting for all the polymers follows the same trends found for the conductivities of the doped polymers; i.e., the more highly conductive polymers display the largest splitting. It is difficult to explain this correlation in terms of structural phase changes when the presumably isostructural polymers described herein display such different electrochemical responses.

Separated waves in systems containing multiple-redox centers have been observed previously in the work with mixed-valence dimers.[18] In these systems, it is believed that electronic interactions, electrostatic and resonance as mediated by the bridging ligand, lead to the observed separation in the waves. It is possible that a similar phenomenon is responsible for the electrochemical splitting in our polymers. At present, this point must remain unresolved.

**Spectroscopic Studies.** In addition to the important inferences regarding structure and chain length, optical studies can provide information concerning the electron-transport properties of conducting solids.[43] Such studies do not suffer from the interparticle and interchain resistance limitations that bulk conductivity measurements do. In order to probe the optical properties associated with conduction electrons, it is first necessary to assign the electronic transitions associated with the monomeric building blocks. Figure 7 depicts the optical absorbance spectra of Ru(II) and Ru(III) octaethylporphyrin bis(pyrazine) monomers, (a) and (b), respectively, and the neutral and partially oxidized $\mu$-pyrazine polymers, (c) and (d), respectively. All four spectra in the visible region display three strong $\pi \rightarrow \pi^*$ absorptions typical of sym-

(41) During the first oxidative trace, a small anodic current was observed for the material which had already been chemically oxidized ($\rho$ = 1.0). Apparently this small current flow represents a small fraction of the polymer that was not oxidized during the chemical treatment and suggests that a more correct formulation for the analyte should have been $[Os(OEP)(pyz)(PF_6)_{0.95}]_n$.

(42) (a) Shacklette, L. W.; Murthy, N. S.; Baughman, R. H. *Mol. Cryst. Liq. Cryst.* **1985**, *121*, 201–209. (b) Baughman, R. H.; Shacklette, L. W.; Murthy, N. S.; Miller, G. G.; Elsenbaumer, R. L. *Mol. Cryst. Liq. Cryst.* **1985**, *118*, 256–261. (c) Baughman, R. H.; Murthy, N. S.; Miller, G. G.; Shacklette, L. W. *J. Chem. Phys.* **1983**, *79*, 1065–1074.

(43) (a) Torrance, J. B.; Scott, B. A.; Welber, B.; Kaufman, F. B.; Seiden, P. E. *Phys. Rev. B* **1979**, *19*, 730–741. (b) Tanner, D. B., in ref 2e, Vol. 2, Chapter 5, pp 205–258.

(44) Gouterman, M. In *The Porphyrins, Physical Chemistry Part A*; Dolphin, D., Ed.; Academic: New York, 1978; Vol. III, Chapter 1.

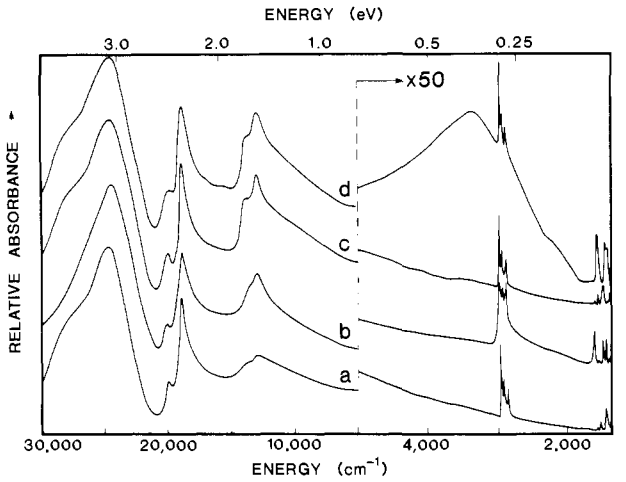


**Figure 7.** Overlay of the visible and near- and mid-infrared absorption spectra of (a) $Ru^{II}(OEP)(pyz)_2$, (b) $Ru^{III}(OEP)(pyz)_2(PF_6)$, (c) $[Ru(OEP)(pyz)]_n$, and (d) $[Ru(OEP)(pyz)I]_n$. Spectra were recorded as Fluorolube mulls, have been normalized to the same porphyrin content, and have been offset for clarity.

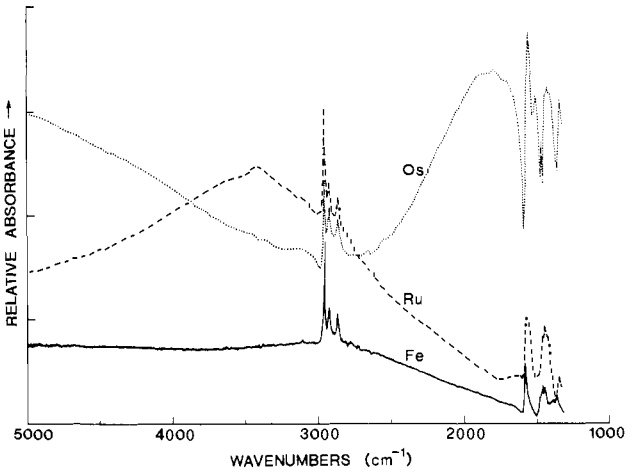


**Figure 8.** Mid-infrared absorption spectra of $[Fe(OEP)(pyz)(PF_6)_{1/3}]_n$ (—), $[Ru(OEP)(pyz)I]_n$ (---), and $[Os(OEP)(pyz)I]_n$ (···) displaying the transition-metal dependence of the mixed-valence spectra. Spectra were recorded as Fluorolube mulls, have been normalized to the same porphyrin content, and have been presented with no offset in the y axis.

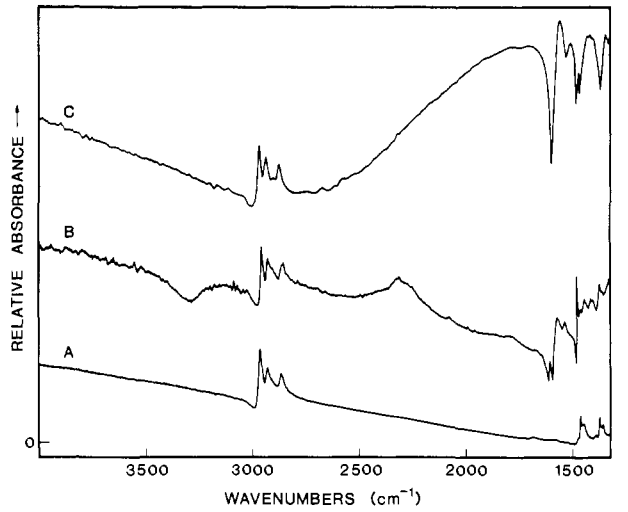


**Figure 9.** Mid-infrared absorption spectra for the series $[Os(OEP)(L\text{-}L)(PF_6)_{1/3}]_n$ where (A) L-L = dabco, (B) L-L = 4,4′-bipyridine, and (C) L-L = pyrazine displaying the ligand dependence of the mixed-valence transition. Spectra were recorded as Fluorolube mulls, have been normalized to the same porphyrin content, and have been offset along the *y* axis for clarity.

metrical metalloporphyrins.[44] The bands found near 13 000 $cm^{-1}$ (1.6 eV) are absent in the spectra of normal four-coordinate metalloporphyrins such as Ni, Cu, and Zn and may be tentatively assigned ruthenium ($d\pi$) to porphyrin ($\pi^*$) charge-transfer (CT) transitions or to doubly excited state of the porphyrin ring.[45] Additional CT bands, Ru ($d\pi$) → pyrazine ($\pi^*$), would be expected in the visible region[46] but are hidden by the very strong porphyrin-based transitions. The dramatic similarities found in the UV–vis/near-IR portion of Figure 7 suggest that the local environments around the porphyrin macrocycles of the monomers and polymers are similar and that oxidation of these complexes does not appreciably alter the electronic distribution in the porphyrin $\pi$ system. Further evidence is thus provided for metal core oxidation.

Normal vibrational spectral features for metalloporphyrin complexes[47] are seen in the infrared region for the Ru(II) and Ru(III) bis(pyrazine) monomer and the neutral polymer, curves a, b, and c, respectively. In curve d, however, the partially oxidized polymer displays a broad, intense absorption centered at 3400 $cm^{-1}$ which is absent in the other spectra. We assign this band to a transition that promotes electron transfer between different metal valence states (mixed-valence or intra band). Bands of this type are often found to be a signature of conductive polymers.[43a]

The origin of mixed-valence transitions in low dimensional conductors has been controversial.[43a,b,48] Because of the similarities of some of these materials to conventional metals, analysis of the optical properties of low dimensional solids has often been treated in the same context as conventional metals employing the Drude "free electron" model.[49] Within the framework of this model, free electron absorption occurs in a metal when the motion of the metallic electrons is influenced by electromagnetic radiation. High metallic reflectivity and the appearance of a Drude-like edge in the reflectance spectra of some low dimensional solids provide evidence for this type of behavior and some rationale for the application of this theory. There is, however, strong evidence that the conduction electrons in many molecular materials are not completely free but are subjected to strong Coulombic interactions.[50] The Drude–Lorentz model[49] takes into account such interactions and can be employed to provide important information concerning the relative electron-transport properties of the conduction electrons in these materials.

The Drude–Lorentz model holds that smaller peak width and larger integrated intensity in this absorption are associated with more highly delocalized electronic states. With this in mind, an assessment of the relative electron-transport properties in the doped Fe, Ru, and Os $\mu$-pyrazine polymers can be made from an analysis of their mixed-valence spectra (Figure 8). The extreme weakness of this transition for the Fe polymer is consistent with only a small degree of delocalization. The stronger and narrower absorption of the ruthenium analogue reveals more pronounced delocalization. The Os congener, on the other hand, displays stronger and narrower absorption which extends into the far-IR, suggestive of the presence of highly delocalized conduction electrons.

Bridging ligand dependence of the mixed valence transition for the series $[Os(OEP)(L\text{-}L)(PF_6)_{1/3}]_n$ is shown in Figure 9. With L-L equal to dabco (curve a, Figure 9), very little electronic absorption attributable to the mixed-valence state is found in the

(45) Antipas, A.; Buchler, J. W.; Gouterman, M.; Smith, P. D. *J. Am. Chem. Soc.* **1978**, *100*, 3015–3024.
(46) Ford, P.; Rudd, R.; Gaunder, R.; Taube, H. *J. Am. Chem. Soc.* **1968**, *90*, 1187–1194.
(47) (a) Alben, J. O. In *The Porphyrins, Physical Chemistry Part A*; Dolphin, D., Ed.; Academic: New York, 1978; Vol. III, Chapter 7. (b) Ogoshi, H.; Saito, Y.; Nakamoto, K. *J. Chem. Phys.* **1972**, *57*, 4194–4202.
(48) Kamaras, K.; Grüner, G.; Sawatzky, G. A. *Solid State Commun.* **1978**, *27*, 1171–1175.
(49) Wooten, F. *Optical Properties of Solids*; Academic: New York, 1972; Chapters 3, 4.
(50) Torrance, J. B. In *Chemistry and Physics of One-Dimensional Metals*; Keller, H. J., Ed.; Plenum: New York, 1977; pp 137–166.

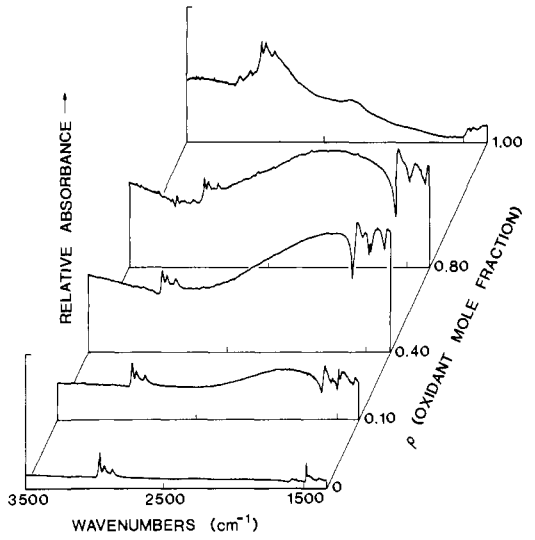


Figure 10. Mid-infrared absorption spectra of $[Os(OEP)(pyz)(PF_6)_\rho]_n$ recorded as a function of dopant [ferricinium hexafluorophosphate] mole fraction, $\rho$. All spectra represent the same porphyrin content and were recorded as Fluorolube mulls.

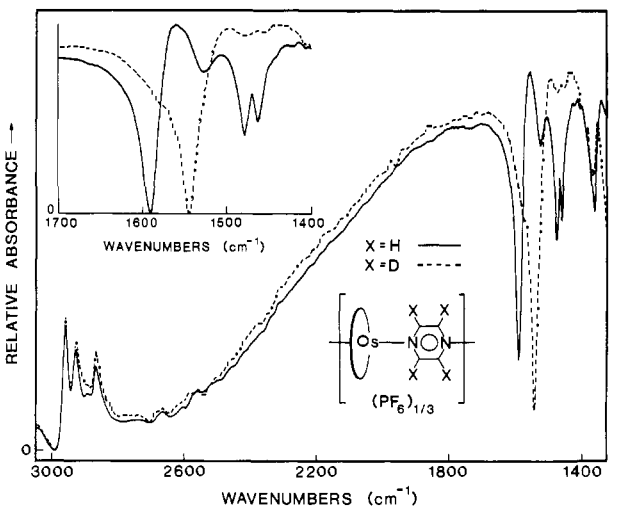


Figure 11. Mid-infrared absorption spectra of $[Os(OEP)(pyz)(PF_6)_{1/3}]_n$ for both pyrazine (—) and pyrazine-$d_4$ (---) displaying the frequency shift in the antiresonance which occurs upon isotopic substitution at the bridging ligand. Inset is an expansion of the region near the antiresonance.

IR, near-IR, or visible (higher energy regions are not shown in this figure). This is not surprising in view of the saturated nature of the bridging ligand. Pyrazine shows the strongest absorption and 4,4′-bipyridine intermediate behavior (curves c and b, respectively).

Dependence of the mixed-valence transition on the oxidant mole fraction, $\rho$, is shown in Figure 10 for the series $[Os(OEP)(pyz)(PF_6)_\rho]_n$. Within this series of stacked spectra, the highest extinction coefficient occurs at $\rho = 0.4$–$0.8$ tailing off on either side of these values. The parallel behavior of conductivity and intervalence optical transitions with respect to transition metal (Table II and Figure 8), bridging ligand (Figure 9 and Table II), and oxidant mole fraction (Figures 3 and 10) supports our contention that these two methods reflect the same phenomenon.

An additional interesting feature of the mixed-valence transition for doped samples of $[Os(OEP)(pyz)]_n$ and $[Os(OEP)(pyz\text{-}d_4)]_n$ shown in Figure 11 is the presence of a prominent antiresonance at 1580 $cm^{-1}$ for [Os(OEP)(pyz)] and 1532 $cm^{-1}$ for the pyz-$d_4$ analogue. The frequency of these antiresonances agrees well with the infrared silent pyrazine breathing modes ($\nu_{8a}$) listed in Table I. A coupling between the mixed-valence transition and a pyrazine vibration is thus implicated. Interactions of conduction electrons with intramolecular vibrations in low dimensional conductors have been considered theoretically by Rice et al.[51] Antiresonances of this type will result when totally symmetric vibrational modes overlap with an electronic continuum. Electron-molecular-vibration coupling has been observed previously in studies of TTF–TCNQ (tetrathiafulvalene–tetracyanoquinodimethane).[43b,51b] The isotopic shift of the antiresonance observed herein confirms the assignment of the coupled mode to the totally symmetric $\nu_{8a}$ mode of pyrazine and provides direct evidence for the participation of this bridging ligand in the conduction process. As far as we are aware, these data represent the first direct experimental evidence for the participation of the bridging ligand in the conduction process of a coordination polymer of this type and serves as an important step in the elucidation of the conduction process in such materials.

## Conclusion

In this paper we reported the conductive, electrochemical, and optical properties of Fe, Ru, and Os octaethylporphyrin coordination polymers bridged by dabco, bpy, and pyz. From the infrared studies chain lengths of these polymers were estimated from an end group analysis, and assignments of the principal vibrational modes were made with the aid of isotopic substitution studies. Partial oxidation of these polymers with a wide variety of oxidants leads to substantial increases in their electrical conductivities relative to the undoped polymers and monomers. Once doped, the conductivities of the polymers derived from different combinations of the constituent metal and bridging ligand follows the trends Os > Ru > Fe and pyrazine > bpy > dabco. Both of these trends are readily explained in terms of increased overlap between the metal d$\pi$ and the bridging ligand $\pi^*$ and resultant increase in electron delocalization among the metal centers. Electrochemical studies of the polymers reveal the presence of metal-centered anodic waves at potentials much less positive than is required for the first ring oxidation of the porphyrin. The metal centers are thus implicated in the conduction pathway for these polymers. Some of the polymers display an interesting splitting of this metal-centered wave, which increases with increasing bridging ligand–metal overlap. The origin of this splitting is not completely understood at this time. Optical studies of the polymers reveal the appearance of a mixed-valence transition which accompanies the doping of these materials. From the characteristics of this transition, inferences have been drawn concerning the relative electron-transport properties in the doped polymers were made. Conclusions generated from the analysis of these transitions concerning the metal, bridging ligand, and oxidation mole fraction are consistent with those derived from the pressed powder conductivity measurements. Furthermore, the appearance of antiresonances in the IR spectra of doped samples of $[Os(OEP)(pyz)]_n$ suggests that the bridging ligand also participates in the conduction process.

**Acknowledgment.** We wish to thank Professors Royce Murray, Tobin Marks, Henry Taube, and Nathan Lewis and Dr. Laughlin McCullough for their helpful discussions and Matthew B. Zisk for his helpful comments on the manuscript. This work was initiated with support from the Center for Materials Research at Stanford University under the NSF-MRL Program, Grant NSF DMR 83-16982-A1. Subsequent support for this work was provided by the National Science Foundation (Grant NSFCHE83-18512) and the Department of Energy (DEFG03-86-45245). NMR spectra were recorded on an instrument supported by the National Science Foundation (Grant CHE81-09064).

(51) (a) Rice, M. J.; Duke, C. B.; Lipari, N. O. *Solid State Commun.* **1975**, *17*, 1089–1093. (b) Rice, M. J.; Lipari, N. O. *Phys. Rev. Lett.* **1977**, *38*, 437–439.